

Anthony Medellin

Department of Engineering Technology & Industrial Distribution, Texas A&M University, College Station, TX 77843 e-mail: antmedellin@tamu.edu

Wenchao Du

Mem. ASME
Department of Industrial & Systems Engineering,
Texas A&M University,
College Station, TX 77843
e-mail: wenchaodu@tamu.edu

Guanxiong Miao

Department of Mechanical Engineering, Texas A&M University, College Station, TX 77843 e-mail: gm2666@tamu.edu

Jun Zou

Department of Electrical & Computer Engineering, Texas A&M University, College Station, TX 77843 e-mail: junzou@tamu.edu

Zhijian Pei

Fellow ASME
Department of Industrial & Systems
Engineering,
Texas A&M University,
College Station, TX 77843
e-mail: zjpei@tamu.edu

Chao Ma¹

Mem. ASME
Department of Engineering Technology &
Industrial Distribution;
Department of Industrial & Systems Engineering;
Department of Mechanical Engineering,
Texas A&M University,
College Station, TX 77843
e-mail: cma@tamu.edu

Vat Photopolymerization 3D Printing of Nanocomposites: A Literature Review

Nanocomposites have been widely used to improve material properties. Nanoscale reinforcement materials in vat photopolymerization resins improve the hardness, tensile strength, impact strength, elongation, and electrical conductivity of the printed products. This paper presents a literature review on the effects of reinforcement materials on nanocomposite properties. Additionally, preprocessing techniques, printing processes, and postprocessing techniques of nanocomposites are discussed. The nanocomposite properties are summarized based on their applications in the mechanical, electrical and magnetic, and biomedical industries. Future research directions are proposed to improve the material properties of printed nanocomposites. [DOI: 10.1115/1.4044288]

Keywords: nanocomposites, stereolithography, vat photopolymerization, 3D printing, material properties

1 Introduction

Additive manufacturing (AM) allows complex geometrical designs to be created without added tooling costs. It also allows small changes in design to be done without adding manufacturing cost. Another benefit of AM is the ability to print end-use parts with minimized material consumption. The ASTM standard [1] divides AM into seven categories, including vat photopolymerization, binder jetting, directed energy deposition, material extrusion, material jetting, powder bed fusion, and sheet lamination. Unique features of vat photopolymerization include the highest resolution and smoothest surface finish of all additive manufacturing processes.

One of the drawbacks of vat photopolymerization is the limited choice in materials since the feedstock resin has to be photopolymerizable. This limits the application space of the printed parts. In order to print materials with various properties and expand the application space, nanoscale reinforcement materials have been added to the base resin to form nanocomposites. Through the incorporation of nanoscale reinforcement materials, properties such as tensile strength, elastic modulus, hardness, and electrical conductivity can be improved.

This review paper focuses on different resins and nanoscale reinforcements that have been used to print nanocomposites. It also covers preprocessing techniques, common printer setups, corresponding printing processes, and postprocessing techniques. The nanocomposite properties, including mechanical, electrical and magnetic, and biomedical, are discussed based on the different application areas. Finally, future directions are proposed to improve equipment and feedstock materials.

2 Feedstock Material

The feedstock material for printing a nanocomposite by vat photopolymerization is a suspension with nanoscale reinforcements suspended in a photopolymer resin. The resin forms the

¹Corresponding author.

Contributed by the Manufacturing Engineering Division of ASME for publication in the JOURNAL OF MICRO- AND NANO-MANUFACTURING. Manuscript received March 28, 2019; final manuscript received July 8, 2019; published online October 1, 2019. Assoc. Editor: Shih-Chi Chen.

matrix of the resultant nanocomposite, while the reinforcements help to achieve desired properties for the targeted application.

2.1 Resins. The resin consists of monomers, oligomers, photoinitiators, diluents, and other additives. The monomers and oligomers are the basis of the resin, which get polymerized and crosslinked when exposed to ultraviolet (UV) light. Photoinitiators decompose after exposure to light and become reactive. Next, the decomposed photoinitiators polymerize certain functional groups of the monomers and oligomers. The photoinitiator needs to be chosen according to the wavelength of the light source. Diluents are used to decrease the viscosity of the resin. This is especially important with the incorporation of reinforcements in a resin as the reinforcements increase the viscosity. Other additives include pigments, chain transfer agents, coupling agents, etc. [2]. Pigment gives color to the polymer, while the chain transfer agent controls the amount of crosslinking in the polymer [3], and the coupling agent improves the bond between the reinforcement material and the resin [4]. The resins that have been studied are listed in Table 1. The material selection for vat photopolymerization is limited. Research of nanocomposites is dominated by acrylates.

Different monomers can be mixed together to tailor the material properties. For example, in the experiment performed by dos Santos et al. [37], multiacrylate monomers (45–50%) and epoxies (15–25%) were used to improve the hardness and Young's modulus of the nanocomposite with carbon nanotubes (CNTs). Most of the nonacrylate or nonepoxy resins have an acrylate end-group functionalization. This functionalization makes the resin capable of being photopolymerized. Geven et al. [34], for instance, used an acrylate end-group for functionalization of poly(trimethylene carbonate) (PTMC). Similarly, acrylate was also used to functionalize poly(D,l-lactide) (PDLLA) [30].

The type of resin that should be chosen depends on the target application and the compatibility with the reinforcement material. Materials with similar refractive indexes, such as acrylate-based resin and silica, can be combined together to limit the Van der Waals attraction [5]. Matching the refractive indexes can also improve the transparency of the slurry, and thus leading to higher resolution. This is because light scattering increases in less transparent resins, causing a decrease in resolution due to unwanted exposure of nearby monomers [5].

2.2 Reinforcements. Reinforcements affect the material properties and therefore the applications of the nanocomposite. The nanoscale reinforcements that were studied are listed in Table 2. The majority of nanocomposites studied use nanoparticles as the reinforcement material. The most studied reinforcement materials are silica nanoparticles, CNTs, and graphene oxide nanoplatelets. Of these reinforcement materials, silica is the most researched for use in nanocomposites. The mechanical properties, especially tensile strength, of nanocomposites are studied more than their biomedical and electrical properties.

2.3 Viscosity of Feedstock. Viscosity is a very important property of the feedstock. If the viscosity is too high, it will not

Table 1 Resins used for 3D printing of nanocomposites by vat photopolymerization

Resin	Reference
Acrylate	[4–26]
Epoxy	[27–29]
Poly(D,l-lactide) (PDLLA)-acrylate	[30,31]
Polypropylene fumarate (PPF)	[32,33]
Poly(trimethylene carbonate) (PTMC)-acrylate	[34]
Polyvinylsilazane (PVSZ)-acrylate	[35]
Vinylpyrrolidone (VP)	[36]

evenly fill the void created after the curing of the former layer and the movement of the build platform. Defects in the part will result from uneven filling. Additionally, a higher viscosity will lead to a longer print time as the resin will take longer to reflow to form a new uniform layer [6]. Diluents can be used to help reduce the viscosity of the resin. Moreover, increasing the temperature also leads to a decrease of the viscosity [5].

Parameters that affect the feedstock viscosity include the shear rate for testing and the amount and material of the reinforcement, as shown in Fig. 1. As shear rate increases, the viscosity decreases for different suspensions. Weng et al. [7] studied the effect of shear rate on acrylate-based resins containing 10 wt % silica nanoparticles, attapulgite (ATP) nanorods, and organically modified montmorillonite (OMMT) nanoplatelets. At a low shear rate of 20 Hz, the viscosity values for the silica-filled, ATP-filled and the OMMT-filled resins were 0.56 Pa·s, 1.7 Pa·s, and 0.78 Pa·s, respectively. At a shear rate of 1000 Hz, the viscosity values achieved were 0.46 Pa·s by the silica, 0.36 Pa·s by the ATP, and 0.33 Pa·s by the OMMT. As the shear rate increased, the nanoparticles deaggregated, the nanorods became oriented along the direction of the shear force, and the nanoplatelets became stacked.

The shelf life of the suspension can be determined by the viscosity [8]. As the suspension ages, the viscosity increases, which depends on the reinforcement material and the filler amount. Larger reinforcement amounts cause a greater increase in viscosity over time, which can be related to the agglomeration of the reinforcement material. To overcome this problem, new resin should be added to dilute the old resin to reduce its viscosity.

3 Preprocessing

Nanoscale reinforcements tend to agglomerate due to their interparticle forces. The agglomeration can lead to nonuniformity and degradation of the reinforcements. Mixing is a crucial preprocessing step to homogeneously disperse the reinforcement into the resin and avoid agglomeration.

There are different ways to mix the reinforcement material in the matrix [3]. Frequently used methods include manual mixing, magnetic stirring, and sonication. Specifically, manual mixing uses a blade that stirs the mixture, and a high rotation speed is needed to help reduce the mixing time. Magnetic stirring is similar to manual mixing, in which a magnetic rod rotates at a high speed to create a homogenous mixture. Both of these methods are economical in terms of the mixing step [3]. However, they can cause air bubbles in the resin, which will reduce the achievable resolution and cause defects in the final part. A vacuum is often used after stirring to help remove air bubbles from the mixture and reclaim solvents. Weng et al. [7] used a planetary vacuum gravity mixer to remove air bubbles that were created during the mixing process. Manapat et al. [9] used vacuum evaporation with magnetic stirring to reclaim the acetone. The third commonly used method to mix materials is sonication (<20 kHz) or ultrasonication (>20 kHz), in which sound waves are used to disperse the reinforcement material [27]. This method can also be used inside a vacuum to aid in the air removal.

The suitable mixing method can be determined based on the materials and the particle size. Some high-energy mixing processes can damage the reinforcement material. For example, carbon nanotubes can be damaged by sonication [38]. They can undergo such defects as buckling and bending. The mixing method can also have an effect on the final particle size and distribution. According to Corcione et al. [10], magnetic stirring is better than sonication insofar that it creates a more stable and homogenous dispersion of the nanoparticles in the acrylate-based matrix with boehmite nanoparticles as the reinforcement material. This increase in homogeneity was represented by the smaller standard deviation of the average particle size right after mixing (1.42 nm for sonication and 0.94 nm for magnetic stirring) and over a 30-day period (7.98 nm for sonication and 1.77 nm for magnetic stirring). The stability is demonstrated in the smaller change in

Table 2 Nanocomposites investigated for vat photopolymerization

Reinforcement type	Reinforcement material	Base polymer	Industry	Material properties of interest	Application	Reference
Nanoparticle	Boehmite	Acrylate	Mechanical	Reinforcement material stability and homogeneity	Surface coating	[10]
Nanoparticle	Carbon black (CB)	Acrylate	Mechanical	Hardness, tensile strength	Rapid prototyping	[20]
Nanoparticle	Cellulose nanocrystals (CNCs)	Acrylate	Biomedical	Tensile strength, elongation, fracture energy	Reconstructive surgery	[12]
Nanoparticle	Cellulose nanocrystals (CNCs)	Epoxy	Mechanical	Tensile strength, Young's modulus, storage modulus	Rapid prototyping	[27]
Nanoparticle	Hydroxyapatite (HA)	PDLLA-acrylate	Biomedical	Flexural modulus, flexural strength	Orthopedic surgery	[30,31]
Nanoparticle	Hydroxyapatite (HA)	PPF	Biomedical	Cell adhesion and proliferation	Bone tissue regeneration	[33]
Nanoparticle	Hydroxyapatite (HA)	PTMC-acrylate	Biomedical	Young's modulus, tensile strength, toughness	Orthopedic surgery	[34]
Nanoparticle	Lignin-coated cellulose nano- crystals (L-CNCs)	Acrylate	Mechanical	Tensile strength, Young's modulus, elongation	Tissue engineering	[7]
Nanoparticle	Magnetite	Acrylate	Electrical	Deflection	Magnetic sensors	[26]
Nanoparticle	Organically modified montmorillonite (OMMT)	Acrylate	Mechanical	Glass transition temperature	Rapid prototyping	[7]
Nanoparticle	Polyvinyl pyrrolidone coated gold	PPF	Biomedical	Biocompatibility, optical absorption	Scaffolds for delivery of therapeutic agents	[32]
Nanoparticle	Silica	Epoxy	Biomedical	Hardness, impact strength, tensile strength, flexural modulus	Dental models	[28,29]
Nanoparticle	Silica	Acrylate, PVSZ-acrylate	Mechanical	Curing speed, resin loading capacity, hardness, volumetric shrinkage	Improved resin, rapid prototyping	[5,7,8,19,35]
Nanoparticle	Silver	Acrylate	Electrical	Resistivity, antimicrobial properties	Sensing devices, biomedical applications	[15,18]
Nanoparticle	Silver-coated lead zirconate titanate	Acrylate	Electrical	Dielectric permittivity	Capacitors	[13]
Nanoparticle	Titania	Epoxy	Biomedical	Hardness, impact strength	Dental models	[28]
Nanofiber or nanotube	Alumina	Acrylate	Mechanical	Fiber alignment	Tailored anisotropy, electrical insulation	[4]
Nanofiber or nanotube	Attapulgite (ATP)	Acrylate	Mechanical	Curing speed	Improved resin	[7]
Nanofiber or nanotube	Boehmite	Acrylate	Mechanical	Flexural strength	Manufacturing complex geometries	[6]
Nanofiber or nanotube	Carbon nanotubes (CNTs)	Acrylate	Electrical, biomedical	Conductivity	Printed circuits, neural regeneration	[11,14,23]
Nanofiber or nanotube	Carbon nanotubes (CNTs)	Epoxy-acrylate	Mechanical	Young's modulus, hardness	Aeronautical	[37]
Nanofiber or nanotube	sepiolite	Epoxy	Biomedical	Hardness, impact strength	Dental models	[28]
Nanoplatelet	Calcium phosphate layered silicate (CPLS)	Acrylate	Mechanical	Volumetric shrinkage, Young's modulus	Rapid prototyping, tooling, and manufacturing	[36]
Nanoplatelet	Graphene	VP	Biomedical	Cell metabolic activity	Cell manipulation	[28]
Nanoplatelet	Graphene oxide (GO)	Epoxy	Biomedical	Hardness, impact strength	Dental models	[30]
Nanoplatelet	Graphene oxide (GO)	Acrylate	Mechanical, electrical	Tensile strength, bending strength, impact strength, conductivity	Rapid prototyping	[9,21,22,24]
Nanoplatelet	Molybdenum sulfide	VP	Biomedical	Cell metabolic activity	Cell manipulation	[36]

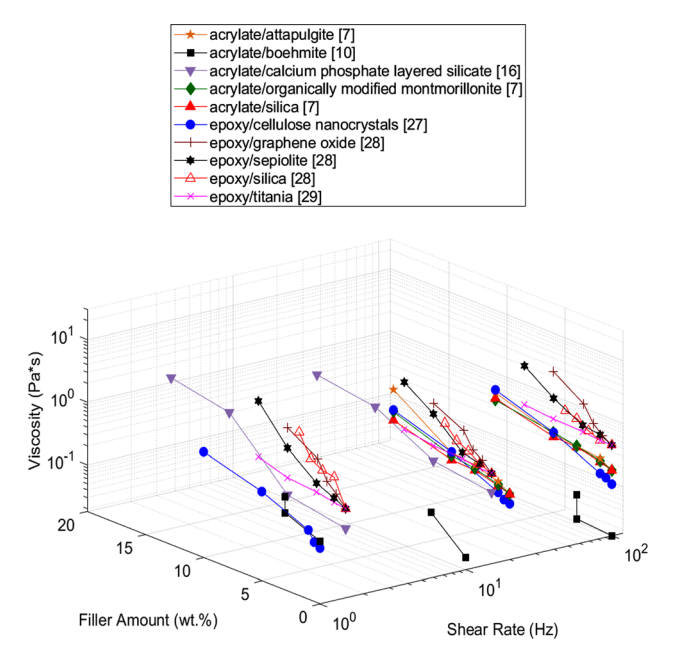


Fig. 1 Effects of reinforcement material and amount on viscosity at different shear rates

particle size over the 30-day period (9.21 nm for sonication and 1.65 nm for magnetic stirring). However, the average size of the sonicated reinforcement particles (69.77 nm right after mixing and 60.56 nm after 30 days) was about 20 nm less than that of the particles which were magnetically mixed (86.07 nm right after mixing and 84.42 nm after 30 days).

Other methods that are used to mix the reinforcement material and the matrix are high-shear homogenization and centrifugation. High-shear homogenization occurs when the mixture flows through a rotor at high speeds. The centripetal force causes the material to flow through the stator, which breaks up the aggregates to produce a homogenized mixture. Gonzalez et al. [11] used high shear homogenization to further disperse CNTs after sonication. Centrifugation can be used to remove large aggregates [36]. After centrifugation, the larger particles migrate to the bottom due to their higher density and then the top part of the centrifuged resin can be used.

Generally, one mixing method can be used in conjunction with others to further facilitate mixing. For example, manual mixing is commonly followed by sonication. Corcione et al. [10] subjected the acrylate-based resins with boehmite nanoparticles to

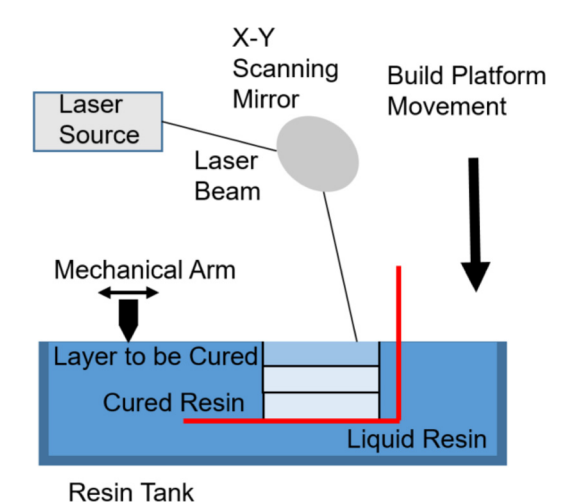


Fig. 2 Top down approach with serial scanning

mechanical mixing, followed by sonication, magnetic mixing, and more mechanical mixing. After preprocessing, it is vital that the mixed resins are stored in a dark environment, which can inhibit the prepolymerization of the resins.

4 Printing Processes

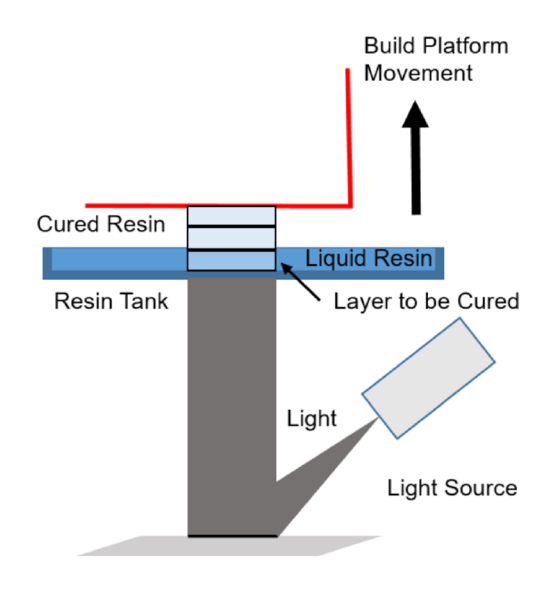
The printing process that should be chosen to create a part depends on the feedstock materials and on the desired printing parameters. The printer used can be classified by the system configuration and the exposure strategy. Within these two main categories, there can be additional components added to the printer to aid in achieving various printing performance.

4.1 System Configurations. There are two main system configurations for a vat photopolymerization printer: top down and bottom up. The difference between the two is the way the build platform moves after a layer is cured. Figure 2 shows a top down approach. In a top down approach, the platform lies in the resin just below the surface. The depth of the build platform in the resin is the layer thickness. After a layer is cured by light exposure, the platform moves toward the bottom of the resin tank to allow for new resin to flow in and the next layer to cure. A mechanical arm can be used to sweep more resin over the previous layer before curing.

The other method is the bottom up approach. This approach is depicted in Fig. 3. The method works by the build platform laying the cure depth away from the bottom of the resin tank. The bottom of the tank is transparent and the light is shone from underneath the resin tank to polymerize the resin. Afterward, the build platform moves upward to allow for more resin to fill in for the next layer [39].

There are many advantages and disadvantages to both system configurations. The top down approach requires much more material compared to the bottom up approach. This leads to an increase in costs and increase in material waste. For this reason, the bottom up approach is more widely used for printing nanocomposites. However, there is not as much stress on the printed part during the printing process for the top down approach, since the bottom layer is not being sheared off after each layer is cured. This advantage can lead to a larger print platform.

4.2 Exposure Strategies. There are two exposure strategies for vat photopolymerization, which are serial scanning and flood



Digital Micromirror Device

Fig. 3 Bottom up approach with flood exposure

exposure. Serial scanning works by running a laser over the resin to selectively polymerize the resin, as is depicted in Fig. 2. In literature, serial scanning is commonly referred to as stereolithography apparatus. Flood exposure, depicted in Fig. 3, selectively casts light on the layer according to the cross section of the part to polymerize the resin. This technique is faster since it is able to polymerize the whole layer simultaneously. This process is commonly referred to as digital light processing.

One parameter related to exposure strategy is layer thickness. The layer thickness should be equal to or less than the cure depth, which is determined by Jacob's equation [40]

$$C_d = D_p \ln(E_{\text{max}}/E_c) \tag{1}$$

where C_d is the cure depth (mm), D_p is the depth of penetration (mm) of the light source into the resin, $E_{\rm max}$ is the exposure energy per unit area (J/cm²), and E_c is the critical exposure energy per unit area (J/cm²).

Delamination is a common issue during printing. It occurs when adjacent layers are not bonded together because the resin does not receive the necessary energy to get fully polymerized [41]. Delamination can be avoided if the layer thickness does not exceed the cure depth. The bonds between the layers become stronger because of overcuring. The drawback of overcuring is a decrease in dimensional accuracy [12].

Layer thickness is also a key factor in part quality and printing speed. Thicker layers allow parts to be printed faster at the expense of the geometrical accuracy and surface smoothness. Smaller layer thicknesses lead to longer print times; however, the parts have a better surface finish and improved geometrical accuracy.

4.3 Serial Scanning Techniques

- 4.3.1 Stereolithography Apparatus. The basic serial scanning technique uses a laser to selectively cure the polymer, which scans the resin through the use of mirrors, as shown in Fig. 2. Lens can be used to help focus the light. This process is able to achieve a resolution of $20 \, \mu m$ [42]. The most commonly used wavelengths are 355 nm and 405 nm. The 405 nm laser is usually more economical [43]. The 355 nm laser is within the range (310–355 nm), where most photoinitiators have maximum absorbance [44].
- 4.3.2 Two-Photon Polymerization. Two-photon polymerization is a type of nanoscale vat photopolymerization with resolution capability of about 100 nm. In the experiment by Zhou et al. [45], a titanium–sapphire laser (780 nm wavelength) was attached to an attenuator to control the power and then the laser beam was expanded to minimize the divergence angle and focused. The laser

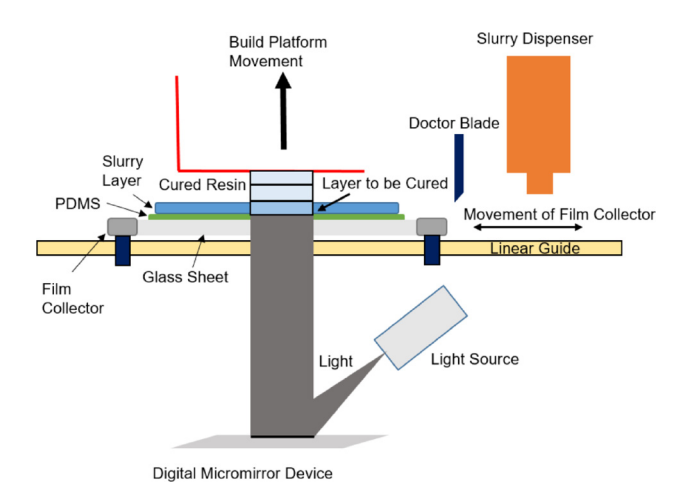


Fig. 4 Projection stereolithography integrated with tape casting

beam is scanned across the surface of the resin using a galvo mirror system to polymerize the resin [46]. This technique greatly improves the printing resolution to 100 nm or less by using a photoinitiator that requires absorption of two photons and ultrashort laser pulses.

4.4 Flood Exposure Techniques

- 4.4.1 Digital Light Processing. This process relies on a digital micromirror device to project different light patterns for different layers to polymerize the resin, as shown in Fig. 3. This method can produce 100 layers in 10 s [43] and has a significantly shorter print time in comparison to the serial scanning technique. Bottom-up digital light processing setup also allows for easy accommodation of fiber alignment mechanisms if needed [4,47].
- 4.4.2 Continuous Liquid Interface Production. This process has an oxygen-permeable window made of a glass membrane, through which ultraviolet images are projected continuously into the resin tank. The glass membrane restricts photopolymerization between the polymer and the resin at the bottom of the tank by oxygenating the resin to create a dead zone. In the dead zone, the oxygen is more prevalent than the free radicals produced by the decomposition of the photoinitiators, so photopolymerization is inhibited. Outside of the dead zone, free radicals are more prevalent and so the photopolymerization of the resin can occur [48]. Out of all the vat photopolymerization techniques, continuous liquid interface production has the highest printing speed [49].
- 4.4.3 Projection Stereolithography Integrated With Tape Casting. Projection stereolithography integrated with tape casting allows resins with high viscosity, which usually stick to the bottom of the resin tank, to be printed through the use of a two-channel sliding design [13], as shown in Fig. 4. The slurry is first dispensed on the polydimethylsiloxane coated glass substrate in thick layers. The thickness is then controlled through movement of the substrate under a doctor blade. Next, the optical mask image, controlled by a digital micromirror device, is projected onto the resin. Eventually, the cured layer is sheared from the polydimethylsiloxane [50].
- 4.4.4 Mask Projected Excimer Stereolithography. Mask projected excimer stereolithography is a process that uses excimer laser irradiation (<300 nm) to polymerize the resin [51]. A pulsed excimer laser with a wavelength of 248 nm and a high peak intensity was used in the experiment to polymerize the resin. Various masks made of chromium or quartz by a laser writer are used with an iris placed in front of the mask. The iris helps to size and select the subportion of the mask to be used. The acrylate used in the experiment had high absorptivity around a wavelength of 200 nm. The two terminating acrylate groups could be polymerized under UV light without photoinitiators. Therefore, this method allows production of biocompatible parts since it does not use photoinitiators, which release toxic substances [51].
- 4.4.5 Projection Microstereolithography Used With Direct Write Cure. Stereolithography can be used in conjunction with other manufacturing processes. Lu et al. [14] used CNTs in an acrylate resin to produce conductive parts. The base of the part was printed using projection microstereolithography and then the extrusion-based direct write cure system was placed on top of the base to print the conductive wire made of CNTs. Next, the resin tank was replaced and printing was continued. The end result was the wires being embedded in the part.

5 Postprocessing

After printing, the part can undergo postprocessing to further increase the material properties. Techniques that are used in the literature include soaking and curing, which will be discussed in the remaining parts of this section.

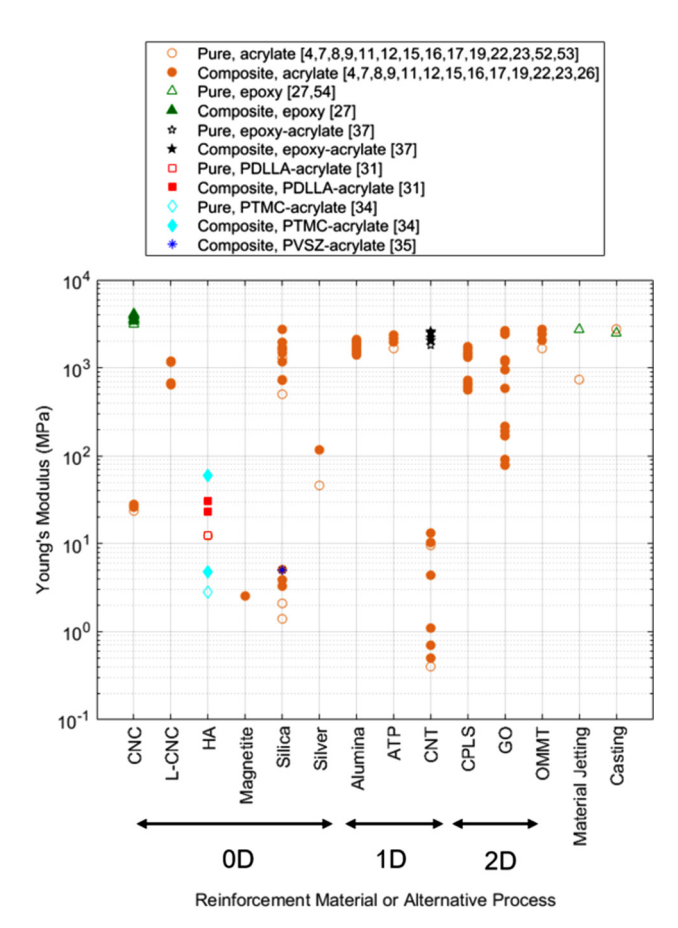


Fig. 5 Achieved Young's modulus in the literature

5.1 Soaking. Soaking removes impurities [12] and unexposed resin [3]. This process is done by rinsing a part several times with a solution or putting a part in an agitated bath. Palaganas et al. [12] soaked the cellulose-nanocrystals-reinforced diacrylate part in phosphate buffered saline to allow the removal of impurities. In a similar way, printed acrylate/GO was soaked in isopropyl alcohol [9]. Silver-reinforced acrylate nanocomposites were soaked in isopropanol hexane in a sonication bath [15], which helped remove uncrosslinked polymer chains. Epoxy-based resins can be soaked in a different solution. For example, tripropylene glycol methyl ether was used to remove unreacted epoxy-based resin [29].

5.2 Curing. Curing allows further polymerization and crosslinking of the part. This process can tailor the properties to the desired values through the control of the temperature or the exposure to various light sources. Exposure to mercury lamps [11], UV light [16], or ovens [17] has showed an improved Young's modulus. Manapat et al. [12] annealed acrylate/GO (1 wt %) samples. The results showed that an annealing at 100 °C for 12 h increased the tensile strength from 91 MPa to 1229 MPa and the modulus from 7.7 MPa to 59.6 MPa. The article states that the increase of properties is due to better cross-linking, removal of water in the part, and smaller pore sizes. Fantino et al. [18] subjected the silver-reinforced acrylate samples to various curing temperatures in air and in a vacuum. The samples that were heated in a vacuum were more electrically conductive compared with those that were heated in air. Moreover, the higher temperatures also led to an increase in electrical conductivity. The drawback of curing is that the parts can undergo warping and shrinkage.

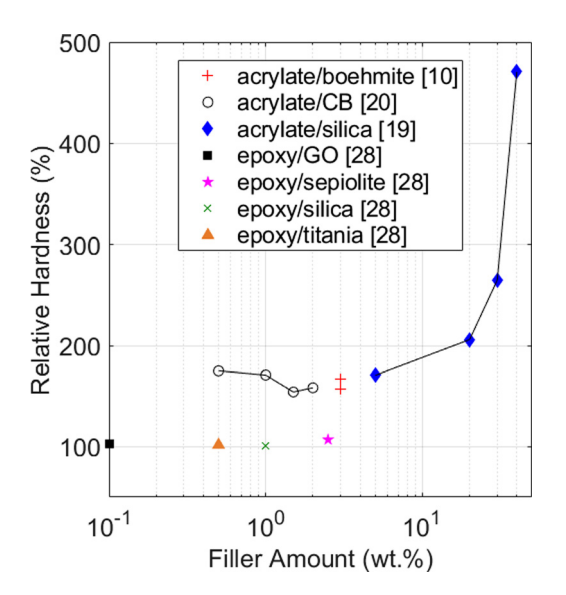


Fig. 6 Effect of filler amount on relative hardness

6 Achieved Properties

The effects of nanoscale reinforcement materials on the material properties of the part are reviewed in this section. The properties are divided into mechanical, electrical and magnetic, and biomedical properties.

6.1 Mechanical. Photopolymers tend to be brittle, especially for acrylate-based ones. Reinforcements have been added to improve the mechanical properties [27]. The improved mechanical properties allow the nanocomposites to be used for more applications. Better properties allow end-use parts to be manufactured, rather than just prototypes. The achievable mechanical properties

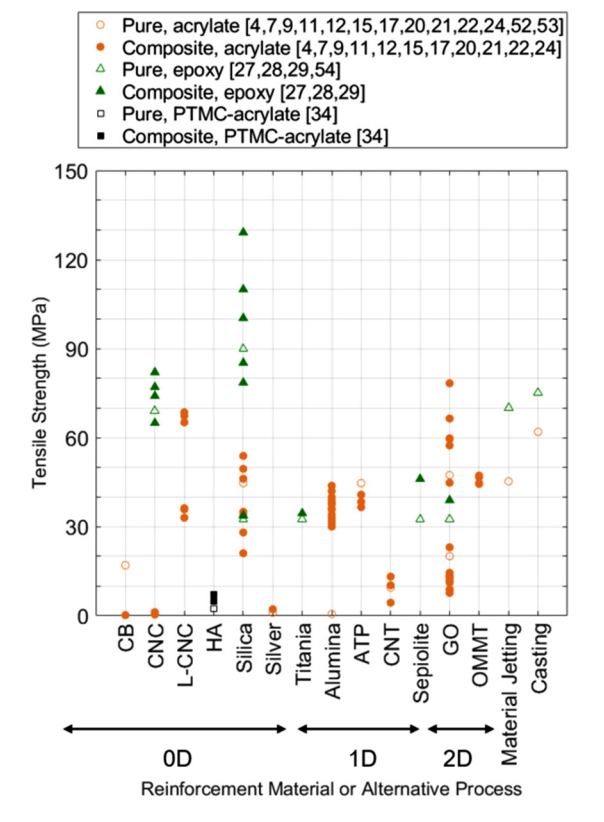


Fig. 7 Achieved tensile strength in the literature

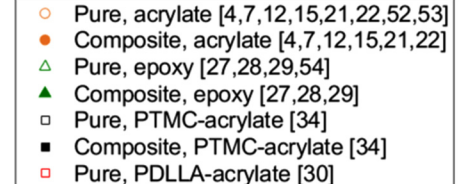
by vat photopolymerization are summarized and compared with those by 3D printing process (i.e., material jetting) and conventional manufacturing process (i.e., casting) [52–54].

6.1.1 Young's Modulus. Young's modulus, also known as elastic modulus, is an important property that helps to determine how the material will respond to external stresses. The addition of reinforcement materials can affect the Young's modulus significantly. For example, OMMT nanoplatelets increase the modulus of an acrylate-based resin from 1660 MPa to 2820 MPa at a 5 wt % filler amount [7]. However, the reinforcement made the nanocomposites more brittle.

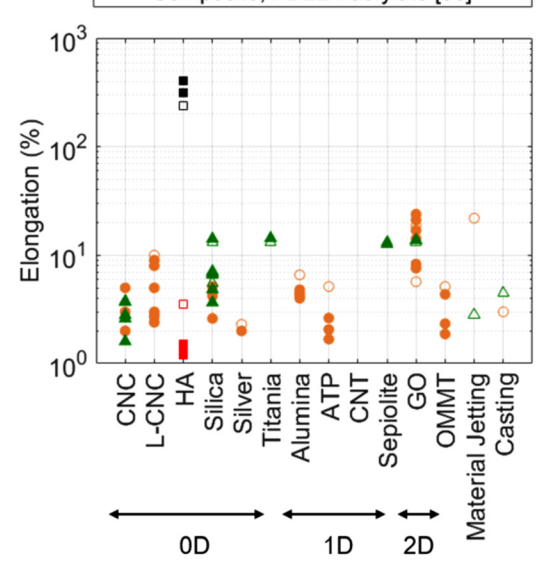
Since mechanical properties of fiber-reinforced nanocomposites depend on the fiber orientation, technique has been developed to help align the fibers during processing. In the work by Yunus et al. [4], a lateral oscillation mechanism was implemented and combined with wall pattern printing technique to generate shear flow to align the aluminum oxide nanofibers (2–6 nm in diameter and 200–400 nm in length) in the acrylate matrix nanocomposites. The elastic modulus and tensile strength were improved by 34% and 28%, respectively, with 1.5 vol % aligned aluminum oxide nanofibers when compared to the base acrylate.

Figure 5 shows the achieved Young's modulus for various reinforcement materials in the literature. The epoxy nanocomposites often have significantly higher Young's modulus over the acrylate nanocomposites because of their stronger base polymer. The best Young's modulus was achieved with the incorporation of cellulose nanocrystals (CNC) in an epoxy-based nanocomposite. With the addition of 3.89 vol % CNC, a value of 4100 MPa was achieved, which is significantly higher than the 3100 MPa of the pure epoxy [27].

6.1.2 Hardness. In the literature, hardness is reported with different scales. Therefore, relative hardness is calculated by dividing the hardness of the nanocomposite by that of the base polymer to illustrate the strengthening effects and compare across different materials. Figure 6 shows the effect of filler amount on relative hardness. As shown in the figure, the effect of



Composite, PDLLA-acrylate [30]



Reinforcement Material or Alternative Process

Fig. 8 Achieved elongation in the literature

reinforcement on hardness is significant in acrylate-based nano-composites reinforced with silica nanoparticles [19]. The hardness increased from 3.4 MPa (pure acrylate-based polymer) to 16 MPa (40 wt % of silica nanoparticles as reinforcement material), which gave a relative hardness of 470%. Carbon black nanoparticles increased the hardness of acrylate-based polymer by 75% at a filler content of 0.5 wt % [20]. The hardness improved from 48 HA for the pure polymer to 84 HA for the nanocomposite.

Epoxy-based nanocomposites are able to achieve high hardness values, even though the effect of reinforcement material is not as significant as in acrylate-based nanocomposites. Wang and Ni [28] achieved a hardness of 122 HRR with 2.5 wt % sepiolite nanorods as reinforcement in an epoxy-based nanocomposite. The increased hardness stems from the higher stiffness of the reinforcement material.

6.1.3 Tensile Strength. Tensile strength is a key mechanical property in the design of products as it helps to determine the load that the part can withstand. Figure 7 shows the effect of reinforcements on tensile strength of nanocomposites. The base resin also plays a key role in the tensile strength, since the polymer bonds of the printed part are the dominant intramolecular force. As a result, epoxy-based nanocomposites tend to have a greater tensile strength compared to acrylate-based ones. The greatest values were achieved with silica in an epoxy-based polymer [29]. At a 2 wt % filler amount, the tensile strength reached 129.1 MPa, compared to the pure polymer value of 89.9 MPa. If too much reinforcement material is added, it will begin to agglomerate, resulting in decreased tensile strength. In the same study by Liu and Mo [29], the highest tensile strength was achieved at 2 wt % silica nanoparticles. At 3 wt %, the tensile strength decreased to 100.3 MPa and continued to decrease for higher concentrations of silica nanoparticles. The highest amount of silica was 5 wt % and had a tensile strength of 78.5 MPa. It should be noted that this is lower than pure polymer value of 89.9 MPa.

6.1.4 Elongation. Elongation at break is a key factor in determining the ductility of a material. As is shown by Fig. 8, elongation is not greatly affected by the addition of reinforcement material. In the literature, the highest elongation was achieved by

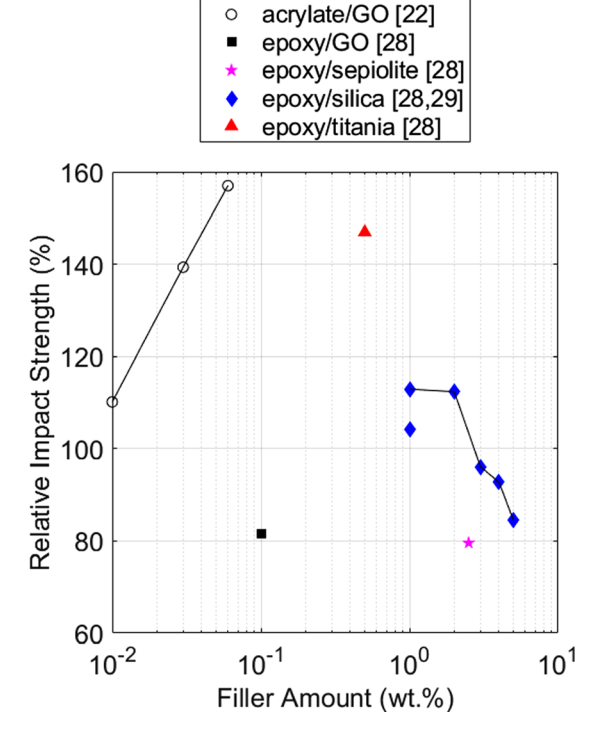


Fig. 9 Effect of filler amount on relative impact strength

SEPTEMBER 2019, Vol. 7 / 031006-7

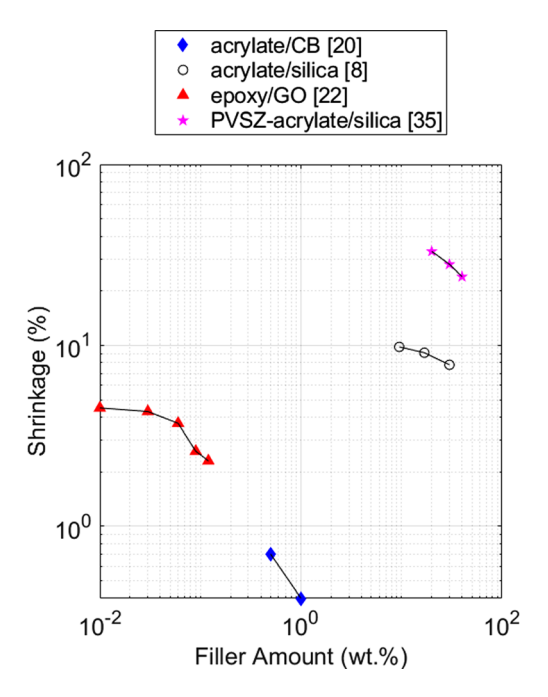


Fig. 10 Effect of reinforcement material on shrinkage

hydroxyapatite (HA) nanoparticles reinforced poly(trimethylene carbonate)—acrylate nanocomposite [34]. Compared with an elongation of 239% for the pure polymer, an elongation of 410% was achieved with the addition of 40 wt % HA.

Elongation is affected by the agglomeration of the reinforcement material. As the amount of nanoscale reinforcement increases, agglomeration becomes more severe [55]. The reinforcement material, if agglomerated, will become areas of concentrated stress that lead to a decrease in elongation [27]. Moreover, the agglomeration of reinforcement material leads to variations in local compositions throughout the material.

The elongation mostly depends on the extent of crosslinking, which further depends on how much energy the resin receives. As the reinforcement amount is increased, less energy reaches the resin since more energy is absorbed and scattered by the reinforcement material. For this reason, nanocomposites with high filler contents have a lower elongation at break compared to those that have small filler contents. In the experiment by Weng et al.

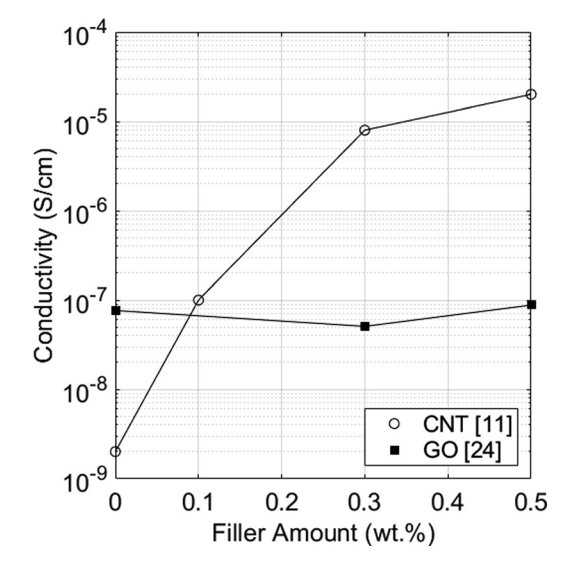


Fig. 11 Effect of reinforcement material and amount on electrical conductivity of acrylate-based polymers

[7], silica nanoparticles, ATP nanorods, and OMMT nanoplatelets were loaded at 1 wt %, 3 wt %, and 5 wt % in the acrylate resin. With the addition of the reinforcement material, the elongation at break was reduced. The pure polymer had a 5.14% elongation at break while the addition of 1 wt % ATP reduced the elongation to 2.63%. The addition of 5 wt % ATP to the resin decreased the elongation at break to 1.68%. As more reinforcement material was added, the elongation at break was further reduced.

Many factors during preprocessing and printing can affect elongation by introducing stress into the printed part. Postprocessing can be done to improve the elongation by minimizing the effects of the induced stresses. Lin et al. [21] printed acrylate/GO (with 0.2 wt %) nanocomposites and cured the samples for 6 h at 60 °C. The elongation increased from 14.2% to 24.0% after curing.

6.1.5 Impact Strength. Impact strength dictates how the material will react to a sudden shock. In the literature, impact strength is reported with different scales. Therefore, relative impact strength is calculated by dividing the impact strength of the nanocomposite by that of the base polymer to illustrate the strengthening effects and compare across different materials. Figure 9 shows the effect of filler amount on relative impact strength. The GOreinforced acrylate-based polymer was able to reach an impact strength of 77.4 J/cm with 0.06 wt % GO [22] while the pure polymer had a value of 49.3 J/cm. Titania nanoparticles improved the impact strength of epoxy by 47% with a 0.5 wt % filler content [28]. The impact strength of 7.2 kJ/m² is a significant improvement over 4.9 kJ/m² for the pure polymer. In a different experiment, silica nanoparticles increased the impact strength of epoxy by 13% at a filler amount of 1 wt % [29] with a maximum value of 4.02 J/m². At higher filler amounts, the impact strength decreases as the silica nanoparticles were rigidly crosslinked in the polymer. This prohibited the nanocomposite from deforming and consequently decreased the impact strength. Similarly, the GO nanoplatelets and sepiolite nanorods decreased the relative impact strength of the pure epoxy.

6.1.6 Geometric Integrity. Geometric integrity is an important factor for additive manufacturing. Parts must be able to have minimal deviations from the nominal shapes and dimensions. Many factors can influence the final geometric shape and dimension of a printed part. Factors such as part thickness, printer settings, curing profile, and reinforcement amount play a role in the final shape of a part. Shrinkage and curling are common effects of the combination of the above stated factors. Curling at the edges of a part is prevalent in samples with a thickness of less than 0.2 mm and samples that are underexposed [26]. Similarly, anisotropic shrinkage can occur if curing is done while the printed part is still attached to the substrate [35]. Figure 10 shows the effect of reinforcement material on shrinkage in printed parts. Shrinkage is influenced by the amount of reinforcement material, because the reinforcement material limits the degree of photopolymerization [22].

6.2 Electrical and Magnetic. Reinforcement materials used to improve electrical and magnetic properties include CNT, GO, silver-coated lead zirconate titanate nanoparticles, and silver nanoparticles. Reinforcements have been shown to improve electrical conductivity, dielectric permittivity, and magnetic intensity. The most researched reinforcement material in the electrical field is CNTs. An application of CNTs is acrylate-based hydrogels that were printed to facilitate nerve regeneration, due to the electrical conductivity of the CNTs and the resembled topography of neural tissues [23].

6.2.1 Electrical Conductivity. Factors that influence electrical conductivity include the material and percentage of the reinforcement. Figure 11 shows how electrical conductivity is affected by the filler amount in acrylate-based nanocomposites. Different studies showed different trends of the effect of the filler amount. For example, as the CNTs in the nanocomposite increased from

 $0\,\mathrm{wt}~\%$ to $1\,\mathrm{wt}~\%$, the electrical conductivity increased from 2×10^{-9} S/cm to 4×10^{-4} S/cm [11]. In another study, however, 0.3 wt % of GO decreased the conductivity and 0.5 wt % increased the electrical conductivity of the nanocomposite [24].

The electrical conductivity of fiber-reinforced nanocomposites depends on the fiber orientation when conductive fibers are used. Greenhall and Raeymaekers used ultrasound transducers for nickel-coated carbon fiber alignment [47]. The resin tank was surrounded by eight ultrasound transducers in an octagonal pattern. The waves produced by the ultrasound transducers caused the fibers to agglomerate at the nodes. The resultant material showed anisotropic electrical conductivity: the resistance between two points with a distance of 1 mm along the fiber direction was 59.7 Ω while that across the fiber direction was 112.7 Ω . A bottom up approach with flood exposure was used, allowing each layer to have a different orientation of fibers to produce functionally complex parts.

Some post-treatments, like an UV exposure and a thermal post-treatment, also affect the electrical conductivity. Chiappone et al. [24] studied how different postprocessing techniques affect the conductivity of nanocomposites. Acrylate/GO (0.3 wt %) nanocomposites were subjected to either a thermal post-treatment at 70 °C for 24 h or a UV light exposure for 1 h [19]. The thermal treatment increased the electrical conductivity of the nanocomposites from 50.8 nS/cm to 109.5 nS/cm, whereas the UV exposure decreased the electrical conductivity to 15.72 nS/cm.

In the experiment by Fantino et al. [18], 15 wt % of silver nitrate (AgNO₃) was incorporated in an acrylate matrix. Postprocessing of the nanocomposites showed that increases in temperature and time allowed for the nanoparticles to increase in size and become more tightly packed. As the temperature increased from 100 to 200 °C, the electrical conductivity increased from 0.22 μ S/cm to 2.4 μ S/cm after 1 h of heat treatment. One thing that should be noted is that the nanocomposite should not be heated to the point where oxidation occurs to avoid a decrease of electrical conductivity. For this reason, a vacuum is usually used to avoid the oxidation and consequently improve the electrical conductivity.

- 6.2.2 Dielectric Permittivity. Dielectric permittivity is the level of electrical polarization a material experiences under an external electric field. The dielectric permittivity of materials is studied for use in capacitors and dielectric resonators. This electrical property can be improved by nanocomposites. Yang et al. [13] improved the dielectric permittivity of the capacitors using silvercoated lead zirconate titanate nanoparticles as the reinforcement material in an acrylate-based resin. The 3D printed capacitor has a specific capacitance of 63 F/g at a current density of 0.5 A/g. The dielectric permittivity increased as the reinforcement amount increased. At 100 Hz, the dielectric permittivity increased from 4 for the pure polymer to 120 with 18 vol % of reinforcement material with a dielectric loss of 0.028. The high dielectric permittivity and low dielectric loss make the nanocomposite a strong candidate for capacitor applications.
- 6.2.3 Magnetic Intensity. The magnetic property of 3D printed parts has been studied for use in microelectromechanical systems. Credi et al. [26] compared the deflection behaviors of two different microcantilevers made of acrylate/magnetite (1 vol %) and pure acrylate plated with magnetic alloy (NiCoP). When a permanent magnet was moved from 20 mm to 19 mm from the cantilever, a 190 μ m deflection was observed by the nanocomposite cantilever and a 115 μ m deflection was observed by the electroless plated cantilever. The results show that the nanocomposite cantilever has larger deflections than the electroless plated cantilever, making this nanocomposite a strong candidate for sensors or actuators.
- **6.3 Biomedical.** Additive manufacturing has a strong capability of creating customized parts [17]. As one of the most prominent applications, the medical field acts as an important driving

factor for the development of printing nanocomposites by the vat photopolymerization process. Many reinforcement materials and resins have been researched for their feasibility in the medical field. Some nanocomposites have good bioactivity and biocompatibility, which allows them to be used for tissue engineering [31].

- 6.3.1 Cell Manipulation. The incorporation of reinforcement material affects the bioactivity of cell culture media. Graphene and molybdenum sulfide were used as the reinforcement materials for a polyvinylpyrrolidone-based polymer to print hydrogels as the media for cell culturing [17]. The reinforcements improved the metabolic activity of the cultured cells. After culturing for 168 h, the nanocomposites showed signs of cell aggregates. The molybdenum sulfide in a polyvinylpyrrolidone-based nanocomposite changed the shape of the endothelial cells from a rounded morphology to a more outstretched morphology. The study contributed this shape change to the different ways of cell adherence. Furthermore, a change in morphology allows the cell to intake more nutrients [56] and thus enables the improvement of the metabolic activity of the cells.
- 6.3.2 Drug Delivery. Nanocomposite scaffolds have been studied for delivery of therapeutic agents. Abdelrasoul et al. [32] used gold nanoparticles coated with polyvinyl pyrrolidone to reinforce polypropylene fumarate for printing scaffolds. The nanocomposite scaffolds can use the nanoparticles to transport the therapeutic agents such as deoxyribonucleic acid or ribonucleic acid. Nanocomposite scaffolds were implanted in mice and removed after 2 weeks. There were no immune responses from the mice. This shows that the mice did not reject the nanocomposite. The inherent inertness and nontoxicity of gold make it an ideal nanofiller for scaffolds that provide a new delivery strategy of drug molecules, large biomolecules, and proteins.
- 6.3.3 Bone Tissue Engineering. Hydroxyapatite (HA, Ca₅(PO₄)₃(OH)) nanopowder was used with dimethacrylate for bone tissue engineering. This nanocomposite can be used to print bone scaffolds for orthopedic surgery. Ronca et al. [31] used HA with PDLLA-acrylate to study how nanocomposite scaffolds affect cell growth. Porous structures were printed to induce bone formation with human marrow mesenchimal cells. The scaffolds allowed cell adhesion and had better results compared to traditional methods. A polypropylene fumarate-based nanocomposite can also be used with HA. The seeded nanocomposite scaffolds showed better cell proliferation than the polymer scaffolds from Day 1 to Day 14 of the study [33].
- 6.3.4 Dental Implants. Sepiolite nanofibers, GO, titania, and silica nanoparticles with an epoxy-based resin can be used in dental applications due to their excellent mechanical properties and biocompatibility [28]. The nanocomposite with sepiolite achieved the highest hardness and tensile strength out of the tested nanocomposites. The printed nanocomposites also achieve high dimensional accuracy. All of these improvements facilitate dental model fabrication.
- 6.3.5 Reconstructive Tissue Surgery. Biocompatible reinforcement materials can be mixed with base resins in tissue engineering to print implants. Cellulose nanocrystals (CNCs) and lignin-coated cellulose nanocrystals (L-CNCs) show potential for use in reconstructive tissue surgery [17]. A human ear was printed with an acrylate-based resin and CNCs as the reinforcement material [12]. The printed ear shows the capability of printed parts to be used in microtia and anotia surgery.

7 Future Directions

7.1 Equipment Improvements. Advances in vat photopolymerization printers are vital to print parts with a high amount of reinforcement materials. The main problems associated with a high amount of reinforcement materials are high viscosity,

uncertainty in exposure parameters, and settling of reinforcement materials from the resin. The problem of high viscosity can be minimized through a temperature control of resins [5]. An increase in resin temperature will decrease the viscosity, which will help to make high-viscosity resins easier to print.

The ideal exposure parameters change significantly with different materials and amounts of reinforcements because of the complex interaction between the light and the reinforcement. An underexposure deteriorates the material properties while an overexposure sacrifices the resolution. It is time consuming to search for the ideal exposure parameters of each nanocomposite material by trial and error. This problem can be solved through an incorporation of an online monitoring and control system that can detect whether a layer is fully polymerized. Moreover, it will also decrease print time, since each layer is given the minimal amount of energy required to be fully polymerized.

The last major problem, settling of reinforcement materials, can be solved through the incorporation of a type of mechanical mixer. Yunus et al. [4] used a lateral oscillation mechanism to align nanowires. The mechanism used shear force to align the nanowires in a specific direction. By adding a similar mechanism to printers, the reinforcement material can be agitated during printing to minimize settling and agglomeration of the reinforcement materials. This type of mechanism is especially important for parts with long print times.

7.2 Material Improvements. Common problems facing printed parts are agglomeration of nanoscale reinforcements and interaction of light and reinforcements. Material research is crucial to improve the achievable properties of printed parts. At high loading amounts, nanoscale reinforcement materials have a tendency to agglomerate, thus reducing the strengthening effects of the reinforcements and increasing the number of defects. Therefore, a high loading of reinforcement materials is currently hard to achieve. Resins that reduce the effects of agglomerations will help to achieve a high loading of reinforcement materials and limit the number of defects in the printed part. This can be achieved through resins that have dispersants.

Reinforcement materials can significantly complicate the lightresin interaction. Without any reinforcements, the light is supposed to interact with the photoinitiator in the resin to start the photopolymerization. However, some reinforcements have a high light absorptivity, hindering the intended interaction between the light and the photoinitiator and thus the photopolymerization of the resin. Also, the nanoscale reinforcements strongly scatter the light, compromising the resolution. Research on novel photoinitiators and reinforcements is needed to maximize the light absorption by the photoinitiators and minimize the light absorption and scattering by the reinforcements.

8 Conclusions

This paper provides a review on printing nanocomposites by vat photopolymerization, which has been increasingly researched during the past decade. Different resins and reinforcement materials are reviewed. Preprocessing methods are investigated, especially their effects on agglomeration and viscosity. Various printing processes are described as well as their use. Effects of different postprocessing techniques are investigated and reported. The properties of the nanocomposites are shown in the areas of mechanical, electrical and magnetic, and biomedical. Finally, future directions to improve equipment and materials are proposed to improve nanocomposites made by vat photopolymerization. The equipment can be improved by incorporating resin vat temperature control to help overcome the increased viscosity from introduction of reinforcement materials, incorporating an online monitoring and control system to detect when a layer is fully polymerized, and incorporating a mechanical mixer to agitate the reinforcement materials to minimize agglomerations and settling. The materials can be improved through research of novel dispersants

that minimize agglomerations. Also, new photoinitiators that have greater absorbance around the wavelength of the light source must be researched to overcome settling of reinforcement materials.

Acknowledgment

This work is supported by the National Science Foundation (NSF) under REU Site Grant (No. EEC 1757882). Any opinions, findings, conclusions, or recommendations presented are those of the authors and do not necessarily reflect the views of the National Science Foundation. We also acknowledge the significant support for summer research and enrichment activities by Texas A&M College of Engineering's Undergraduate Summer Research Grant Program.

Nomenclature

 $AgNO_3 = silver nitrate$

 C_d = cure depth

 $C_d = D_p \ln(E_{\text{max}}/E_c)DNA = \text{deoxyribonucleic acid}$

 $D_p = \text{depth of penetration}$

 \vec{E}_c = critical exposure energy per unit area

 $E_{\rm max} = {\rm exposure\ energy\ per\ unit\ area}$

References

- ASTM, 2015, "Standard Terminology for Additive Manufacturing—General Principles—Terminology," ASTM International. West Conshohocken, PA, Standard No. ISO/ASTM52900-15.
- [2] Ligon, S. C., Liska, R., Stampfl, J., Gurr, M., and Mülhaupt, R., 2017, "Polymers for 3D Printing and Customized Additive Manufacturing," Chem. Rev., 117(15), pp. 10212–10290.
- [3] Manapat, J. Z., Chen, Q., Ye, P., and Advincula, R. C., 2017, "3D Printing of Polymer Nanocomposites Via Stereolithography," Macromol. Mater. Eng., 302(9), p. 1600553.
- [4] Yunus, D. E., Shi, W., Sohrabi, S., and Liu, Y., 2016, "Shear Induced Alignment of Short Nanofibers in 3D Printed Polymer Composites," Nanotechnology, 27(49), p. 495302.
- [5] Wozniak, M., de Hazan, Y., Graule, T., and Kata, D., 2011, "Rheology of UV Curable Colloidal Silica Dispersions for Rapid Prototyping Applications," J. Eur. Ceram. Soc., 31(13), pp. 2221–2229.
- [6] Han, Y., Wang, FKe., Wang, H., Jiao, X., and Chen, D., 2018, "High-Strength Boehmite-Acrylate Composites for 3D Printing: Reinforced Filler-Matrix Interactions," Compos. Sci. Technol., 154, pp. 104–109.
- [7] Weng, Z., Zhou, Y., Lin, W., Senthil, T., and Wu, L., 2016, "Structure-Property Relationship of Nano Enhanced Stereolithography Resin for Desktop SLA 3D Printer," Compos. Part A: Appl. Sci. Manuf., 88, pp. 234–242.
- [8] Gurr, M., Hofmann, D., Ehm, M., Thomann, Y., Kübler, R., and Mülhaupt, R., 2008, "Acrylic Nanocomposite Resins for Use in Stereolithography and Structural Light Modulation Based Rapid Prototyping and Rapid Manufacturing Technologies," Adv. Funct. Mater., 18(16), pp. 2390–2397.
- [9] Manapat, J. Z., Mangadlao, J. D., Tiu, B. D. B., Tritchler, G. C., and Advincula, R. C., 2017, "High-Strength Stereolithographic 3D Printed Nanocomposites: Graphene Oxide Metastability," ACS Appl. Mater. Interfaces 9(11), pp. 10085–10093.
- [10] Corcione, C. E., Cataldi, A., and Frigione, M., 2013, "Measurements of Size Distribution Nanoparticles in Ultraviolet-Curable Methacrylate-Based Boehmite Nanocomposites," J. Appl. Polym. Sci., 128(6), pp. 4102–4109.
- [11] Gonzalez, G., Chiappone, A., Roppolo, I., Fantino, E., Bertana, V., Perrucci, F., Scaltrito, L., Pirri, F., and Sangermano, M., 2017, "Development of 3D Printable Formulations Containing CNT With Enhanced Electrical Properties," Polymers, 109, pp. 246–253.
- [12] Palaganas, N. B., Mangadlao, J. D., de Leon, A. C. C., Palaganas, J. O., Pangilinan, K. D., Lee, Y. J., and Advincula, R. C., 2017, "3D Printing of Photocurable Cellulose Nanocrystal Composite for Fabrication of Complex Architectures Via Stereolithography," ACS Appl. Mater. Interfaces, 9(39), pp. 34314–34324.
- [13] Yang, Y., Chen, Z., Song, X., Zhu, B., Hsiai, T., Wu, P.-I., Xiong, R., Shi, J., Chen, Y., Zhou, Q., and Shung, K. K., 2016, "Three Dimensional Printing of High Dielectric Capacitor Using Projection Based Stereolithography Method," Nano Energy, 22, pp. 414–421.
- [14] Lu, Y., Vatani, M., and Choi, J.-W., 2013, "Direct-Write/Cure Conductive Polymer Nanocomposites for 3D Structural Electronics," J. Mech. Sci. Technol., 27(10), pp. 2929–2934.
- [15] Sciancalepore, C., Moroni, F., Messori, M., and Bondioli, F., 2017, "Acrylate-Based Silver Nanocomposite by Simultaneous Polymerization—Reduction Approach Via 3D Stereolithography," Compos. Commun., 6, pp. 11–16.
- [16] Gurr, M., Thomann, Y., Nedelcu, M., Kübler, R., Könczöl, L., and Mülhaupt, R., 2010, "Novel Acrylic Nanocomposites Containing In-Situ Formed Calcium Phosphate/Layered Silicate Hybrid Nanoparticles for Photochemical Rapid Prototyping, Rapid Tooling and Rapid Manufacturing Processes," Polymers, 51(22), pp. 5058–5070.

- [17] Feng, X., Yang, Z., Chmely, S., Wang, Q., Wang, S., and Xie, Y., 2017, "Lignin-Coated Cellulose Nanocrystal Filled Methacrylate Composites Prepared Via 3D Stereolithography Printing: Mechanical Reinforcement and Thermal Stabilization," Carbohydr. Polym., 169, pp. 272–281.
- [18] Fantino, E., Chiappone, A., Calignano, F., Fontana, M., Pirri, F., and Roppolo, I., 2016, "In Situ Thermal Generation of Silver Nanoparticles in 3D Printed Polymeric Structures," Materials, 9(7), p. 589.
- [19] Chiappone, A., Fantino, E., Roppolo, I., Lorusso, M., Manfredi, D., Fino, P., Pirri, C. F., and Calignano, F., 2016, "3D Printed PEG-Based Hybrid Nanocomposites Obtained by Sol-Gel Technique," ACS Appl. Mater. Interfaces, 8(8), pp. 5627-5633.
- [20] Chiu, S.-H., Wicaksono, S. T., Chen, K.-T., Chen, C.-Y., and Pong, S.-H., 2015, "Mechanical and Thermal Properties of Photopolymer/CB (Carbon Black) Nanocomposite for Rapid Prototyping," Rapid Prototyping J., 21(3), pp. 262-269.
- [21] Lin, D., Jin, S., Zhang, F., Wang, C., Wang, Y., Zhou, C., and Cheng, G. J., 2015, "3D Stereolithography Printing of Graphene Oxide Reinforced Complex Architectures," Nanotechnology, 26(43), p. 434003.
- [22] Li, J., Wang, L., Dai, L., Zhong, L., Liu, B., Ren, J., and Xu, Y., 2018, 'Synthesis and Characterization of Reinforced Acrylate Photosensitive Resin by 2-Hydroxyethyl Methacrylate-Functionalized Graphene Nanosheets for 3D Printing," J. Mater. Sci., 53(3), pp. 1874-1886.
- [23] Lee, S.-J., Zhu, W., Nowicki, M., Lee, G., Heo, D. N., Kim, J., Zuo, Y. Y., and Zhang, L. G., 2018, "3D Printing Nano Conductive Multi-Walled Carbon Nanotube Scaffolds for Nerve Regeneration," J. Neural Eng., 15(1), p. 016018.
- [24] Chiappone, A., Roppolo, I., Naretto, E., Fantino, E., Calignano, F., Sangermano, M., and Pirri, F., 2017, "Study of Graphene Oxide-Based 3D Printable Composites: Effect of the in Situ Reduction," Compos. Part B: Eng., 124, pp. 9-15
- [25] Esposito Corcione, C., Striani, R., Montagna, F., and Cannoletta, D., 2015, "Organically Modified Montmorillonite Polymer Nanocomposites for Stereolithography Building Process," Polym. Adv. Technol., 26(1), pp. 92–98.
- [26] Credi, C., Fiorese, A., Tironi, M., Bernasconi, R., Magagnin, L., Levi, M., and Turri, S., 2016, "3D Printing of Cantilever-Type Microstructures by Stereolithography of Ferromagnetic Photopolymers," ACS Appl. Mater. Interfaces, 8(39), pp. 26332–26342.
- [27] Kumar, S., Hofmann, M., Steinmann, B., Foster, E. J., and Weder, C., 2012, 'Reinforcement of Stereolithographic Resins for Rapid Prototyping With Cellulose Nanocrystals," ACS Appl. Mater. Interfaces, 4(10), pp. 5399–5407.
 [28] Wang, L., and Ni, X., 2017, "The Effect of the Inorganic Nanomaterials on the
- UV-Absorption, Rheological and Mechanical Properties of the Rapid Prototyping Epoxy-Based Composites," Polym. Bull., 74(6), pp. 2063–2079.
- [29] Liu, H., and Mo, J., 2010, "Study on Nanosilica Reinforced Stereolithography Resin," J. Reinf. Plast. Compos., 29(6), pp. 909-920.
- [30] Ronca, A., Ambrosio, L., and Grijpma, D. W., 2013, "Preparation of Designed Poly (D, L-Lactide)/Nanosized Hydroxyapatite Composite Structures by Stereolithography," Acta Biomater., 9(4), pp. 5989-5996
- [31] Ronca, A., Ambrosio, L., and Grijpma, D. W., 2012, "Design of Porous Three-Dimensional PDLLA/Nano-Hap Composite Scaffolds Using lithography," J. Appl. Biomater. Funct. Mater., **10**(3), pp. 249–258.
- [32] Abdelrasoul, G. N., Farkas, B., Romano, I., Diaspro, A., and Beke, S., 2015, "Nanocomposite Scaffold Fabrication by Incorporating Gold Nanoparticles Into Biodegradable Polymer Matrix: Synthesis, Characterization, and Photothermal Effect," Mater. Sci. Eng.: C, 56, pp. 305-310.
- [33] Lee, J. W., Ahn, G., Kim, D. S., and Cho, D.-W., 2009, "Development of Nanoand Microscale Composite 3D Scaffolds Using PPF/DEF-HA and Micro-Stereolithography," Microelectron. Eng., 86(4–6), pp. 1465–1467.

 [34] Geven, M. A., Varjas, V., Kamer, L., Wang, X., Peng, J., Eglin, D., and Grijpma, D. W., 2015, "Fabrication of Patient Specific Composite Orbital Floor Implants
- by Stereolithography," Polym. Adv. Technol., 26(12), pp. 1433–1438.
 [35] Pham, T. A., Kim, D.-P., Lim, T.-W., Park, S.-H., Yang, D.-Y., and Lee, K.-S.,
- 2006, "Three-Dimensional SiCN Ceramic Microstructures Via Nano-Stereolithography of Inorganic Polymer Photoresists," Adv. Funct. Mater., 16(9), pp. 1235-1241.

- [36] Gallardo, A., Pereyra, Y., Martínez-Campos, E., García, C., Acitores, D., Casado-Losada, I., Gómez-Fatou, M. A., Reinecke, H., Ellis, G., Acevedo, D., Rodríguez-Hernández, J., and Salavagione, H. J., 2017, "Facile One-Pot Exfoliation and Integration of 2D Layered Materials by Dispersion in a Photocurable Polymer Precursor," Nanoscale, 9(30), pp. 10590–10595.

 [37] dos Santos, M. N., Opelt, C. V., Lafratta, F. H., Lepienski, C. M., Pezzin, S. H.,
- and Coelho, L. A., 2011, "Thermal and Mechanical Properties of a Nanocomposite of a Photocurable Epoxy-Acrylate Resin and Multiwalled Carbon Nanotubes," Mater. Sci. Eng.: A, 528(13-14), pp. 4318-4324.
- [38] Lu, K. L., Lago, R. M., Chen, Y. K., Green, M. L. H., Harris, P. J. F., and Tsang, S. C., 1996, "Mechanical Damage of Carbon Nanotubes by Ultrasound," Carbon, 34(6), pp. 814-816.
- [39] de Leon, A. C., Chen, Q., Palaganas, N. B., Palaganas, J. O., Manapat, J., and Advincula, R. C., 2016, "High Performance Polymer Nanocomposites for Additive Manufacturing Applications," Reactive Funct. Polym., 103, pp.
- [40] Lee, J. H., Prud'Homme, R. K., and Aksay, I. A., 2001, "Cure Depth in Photopolymerization: Experiments and Theory," J. Mater. Res., 16(12), pp.
- [41] Park, W. S., Kim, M. Y., Lee, H. G., and Cho, H. S., and Leu, M.-C., 1998, "Process Layer Surface Inspection SLA Products," Intell. Syst. Des. Manuf., 3517, pp. 70-79.
- [42] Melchels, F. P., Feijen, J., and Grijpma, D. W., 2010, "A Review on Stereolithography and Its Applications in Biomedical Engineering," Biomaterials, **31**(24), pp. 6121–6130.
- [43] Farahani, R. D., Dubé, M., and Therriault, D., 2016, "Three-Dimensional Printing of Multifunctional Nanocomposites: Manufacturing Techniques and Applications," Adv. Mater., 28(28), pp. 5794–5821.
- [44] Partanen, J. P., 1996, "Solid State Lasers for Stereolithography," Int. Congr. Appl. Lasers Electro-Opt., 1, pp. E115–E123.
- [45] Zhou, X., Hou, Y., and Lin, J., 2015, "A Review on the Processing Accuracy of Two-Photon Polymerization," AIP Adv., 5(3), p. 030701.
- [46] Köhler, J., Ksouri, S. I., Esen, C., and Ostendorf, A., 2017, "Optical Screw-Wrench for Microassembly," Microsyst. Nanoeng., 3, p. 16083.
 [47] Greenhall, J., and Raeymaekers, B., 2017, "3D Printing Macroscale Engineered
- Materials Using Ultrasound Directed Self-Assembly and Stereolithography," Adv. Mater. Technol., 2(9), p. 1700122.
- [48] Janusziewicz, R., Tumbleston, J. R., Quintanilla, A. L., Mecham, S. J., and DeSimone, J. M., 2016, "Layerless Fabrication With Continuous Liquid Interface Production," Proc. Natl. Acad. Sci., 113(42), pp. 11703-11708.
- [49] Balli, J., Kumpaty, S., and Anewenter, V., 2017, "Continuous Liquid Interface Production of 3D Objects: An Unconventional Technology and Its Challenges and Opportunities," ASME Paper No. IMECE2017-71802
- Song, X., Chen, Y., Lee, T. W., Wu, S., and Cheng, L., 2015, "Ceramic Fabrication Using Mask-Image-Projection-Based Stereolithography Integrated With Tape-Casting," J. Manuf. Processes, 20, pp. 456-464.
- [51] Farkas, B., Dante, S., and Brandi, F., 2017, "Photoinitiator-Free 3D Scaffolds Fabricated by Excimer Laser Photocuring," Nanotechnology, 28(3), p. 034001.
- [52] Hsieh, T. H., Kinloch, A. J., Taylor, A. C., and Kinloch, I. A., 2011, "The Effect of Carbon Nanotubes on the Fracture Toughness and Fatigue Performance of a Thermosetting Epoxy Polymer," J. Mater. Sci., 46(23), p. 7525.
- [53] Matweb, 2019, "Overview of Materials for Acrylic, Cast," MatWeb Material Property Data.
- [54] Bass, L., Meisel, N. A., and Williams, C. B., 2016, "Exploring Variability of Orientation and Aging Effects in Material Properties of Multi-Material Jetting
- Parts," Rapid Prototyping J., 22(5), pp. 826–834. [55] Chang, S., Attinger, D., Chiang, F.-P., Zhao, Y., and Patel, R. C., 2004, "SIEM Measurements of Ultimate Tensile Strength and Tensile Modulus of Jetted, UV-Cured Epoxy Resin Microsamples," Rapid Prototyping J., 10(3), pp. 193 - 199
- [56] Young, K. D., 2007, "Bacterial Morphology: Why Have Different Shapes?," Curr. Opin. Microbiol., 10(6), pp. 596-600.